Available online at www.sciencedirect.com
ScienceDirect
Journal of Organometallic Chemistry 693 (2008) 2079–2090
Journal of Organometallic Chemistry
www.elsevier.com/locate/jorganchem

Acceptor substituted *N*-heterocyclic carbenes and their Rh(I)complexes: Synthesis, structure and properties

Agnes Bittermann [a], Peter Härter [a,*], Eberhardt Herdtweck [a], Stephan D. Hoffmann [b], Wolfgang A. Herrmann [a,*]

[a] *Department of Chemistry, Chair of Inorganic Chemistry, Technische Universität München, Lichtenbergstraße 4, 85747 Garching, Germany*
[b] *Chair of Inorganic Chemistry with Focus on Novel Materials, Technische Universität München, D-85747 Garching bei München, Germany*

Received 3 January 2008; received in revised form 27 January 2008; accepted 27 January 2008
Available online 2 February 2008

Abstract

Rhodium(I) complexes of acceptor substituted *N*-heterocyclic carbenes were obtained either by transmetalation from the corresponding Ag(I) complexes or by thermal decomposition of corresponding pentafluorobenzene carbene adducts. All complexes were fully characterized by means of NMR- and mass spectroscopy. Compounds **5**, **6**, **7** and **11** were although characterized by single-crystal X-ray analysis. The relative σ-donor/π-acceptor strength of the NHC ligands was determined by means of IR spectroscopy. Dimerisation behaviour of Rh carbonyl complexes was studied.

Keywords: NHC; Rhodium complexes; σ-Donor/π-acceptor-properties; Dimerisation behaviour

1. Introduction

Since the discovery of *N*-heterocyclic carbenes (NHCs) by Öfele [1], Wanzlick and Schönherr [2] in 1968 and isolation of the first stable free crystalline carbene by Arduengo III et al. [3] in 1991, NHCs gained increasing attention as a new class of ligands used in transition metal compounds [4] and in catalysis [5]. The most unique feature of NHCs is the formation of strong bonds to transition metals. The reason for such behaviour is attributed to a strong σ-donor ability of this ligand class. However, noticeable participation of the π-system of NHCs in the bonding to the metal has recently been proposed on the basis of quantum chemical studies [6]. Modification of electronic properties of NHC ligands in order to improve the performance of molecular catalysts is one of the main areas of our research. Introduction of electron withdrawing substituents or replacement of carbon atoms with electronegative elements in the 4,5-position of the imidazolylidene ring reduces the NHC donor strength. As a result enhanced performance in Heck type CC-coupling reactions is observed [7].

On the other hand NHCs which contain only one heteroatom can react as lewis acids and coordinate small molecules such as CO [8]. Very strong NHC donor ligands can even activate molecules such as hydrogen or ammonia [9].

Only few references referring to 4,5-acceptor substituted imidazol-2-ylidene ligands can be found in the literature. Peris et al. reports synthesis and characterization of 4,5-dichloroimidazolylidene ligands. Rhodium and iridium complexes of these NHCs showed enhanced activity in catalytic hydrosilylation of terminal acetylenes and cyclisation of acetylenic carboxylic acids [10].

We now report a comparative study of NHC ligands **1** (Fig. 1). Interaction of the π-system of the ligand with the metal represents an important goal of this study. Inductive effects and effects achieved by modification of the π-system will be compared in 4,5-dichloro- and 4,5-dicyanoimidazolylidene ligands. Benzyl residues at N-atoms were chosen in order to offer a possible kinetic trap of intermediates by weak interaction of the residue with the metal

* Corresponding authors. Tel.: +49 89 289 13080; fax: +49 89 289 13473 (P. Harter).
E-mail address: lit@arthur.anorg.chemie.tu-muenchen.de (P. Härter).

0022-328X/$ - see front matter © 2008 Elsevier B.V. All rights reserved.
doi:10.1016/j.jorganchem.2008.01.039

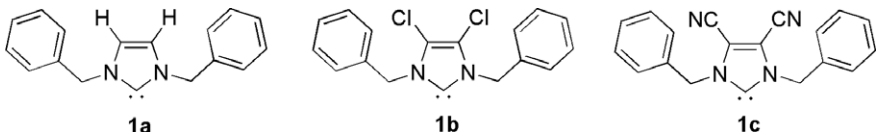

Fig. 1. Carbene ligands.

centre. During preparation of this manuscript Bielawski and coworkers reported the synthesis of similar NHC ligands and their Rh complexes [11].

2. Results and discussion

2.1. Synthesis of ligands

4,5-Dichloro-1-benzylimidazole was obtained in a straightforward way by deprotonation of 4,5-dichloroimidazole with potassium carbonate in acetonitrile and further alkylation with benzyl bromide. Subsequent benzylation of obtained product in toluene with another equivalent of the benzyl bromide yielded 69% of the 4,5-dichloro-1,3-dibenzylimidazoliumsalt **3a** as an air stable white powder (Schemes 1, 2).

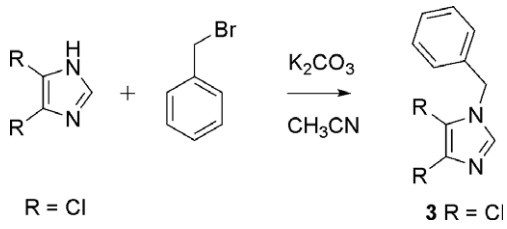

Scheme 1. Synthesis of substituted imidazole **3**.

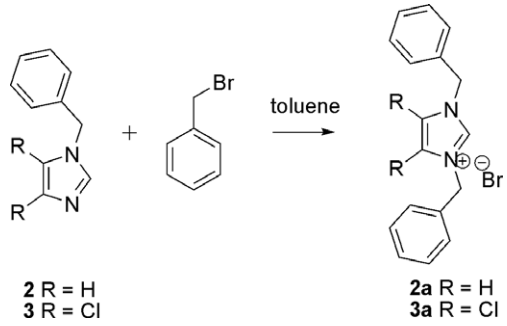

Scheme 2. Synthesis of imidazolium salt **2a** and **3a**.

Synthesis of 4,5-dicyano-1,3-dibenzylimidazol-2-ylidene was successful through a thermal decomposition of compound **4**, a new member of a compound class recently used by Waymouth and Grubbs as a novel source of *N*-heterocyclic carbenes [12]. Corresponding compounds were synthesized by the reaction of *N*,*N*′-disubstituted diamines and pentafluorobenzaldehyde in the presence of a catalytic amount of acetic acid.

In our own synthesis of NHC–pentafluorobenzene adducts, we started with the acyclic commercially available diaminomaleonitrile (DAMN). DAMN was smoothly condensed with benzaldehyde in methanol according to literature procedures [13]. *N*-Benzyl derivate was obtained upon $NaBH_4$ reduction of the resulting Schiff base. The second formation of an imine and further reduction leads to *N*,*N*′-dibenzyldiaminomaleonitrile (Scheme 3). Condensation of this *sec*-diamine with pentafluorobenzaldehyde in acetic acid gave **4** in high yield within 48 h (Scheme 4).

2.1.1. TG-MS/DSC studies of 4

Decomposition of **4** was investigated by thermal gravimetric analysis and differential scanning calorimetry. The corresponding plots are given in Fig. 2. Ten milligrams of the sample were heated from 35 to 700 °C at the rate of 10 K min^{-1}. At the onset temperature of 138 °C a strong exothermic peak occurs. This is accompanied by a sharp increase of the ion current (167 amu) as detected by mass spectrometry (max. at 157.9 °C), which indicates the loss of pentafluorobenzene and formation of carbene **1c**.

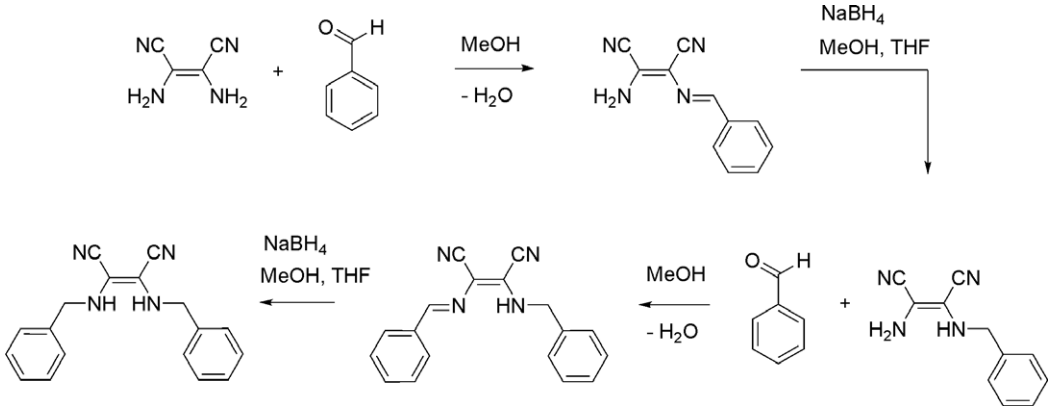

Scheme 3. Synthesis of *N*,*N*′-dibenzyldiaminomaleonitrile [13].

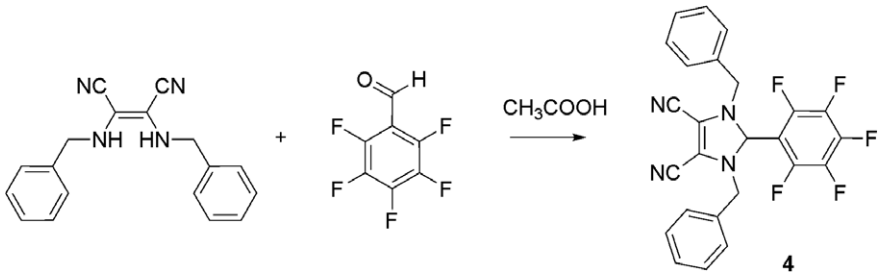

Scheme 4. Synthesis of the NHC precursor **4**.

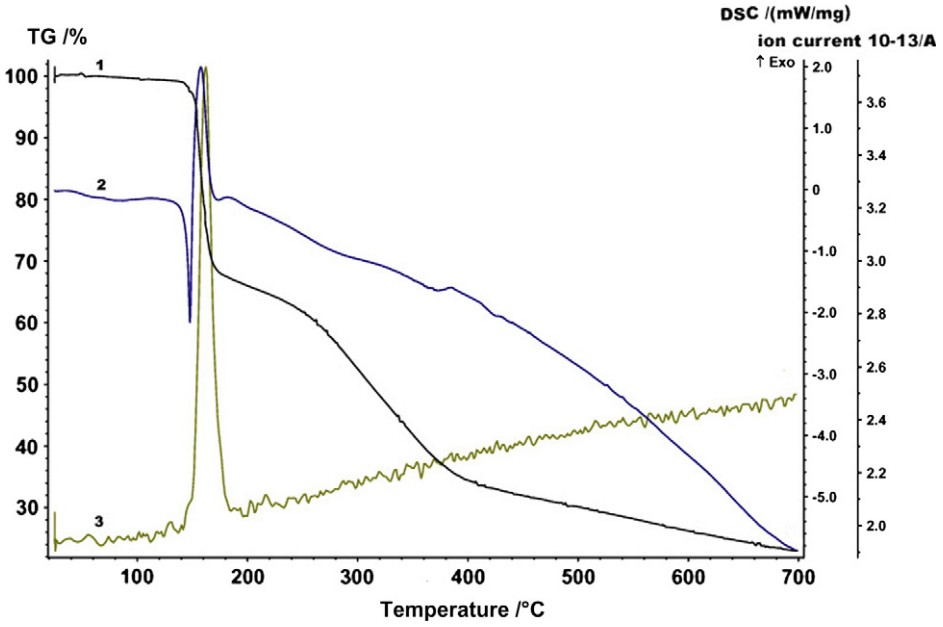

Fig. 2. Thermogravimetric analysis (1), differential scanning calorimetry (2) and mass spectrometric ion current (3, for 167 amu) of compound **4** as a function of the temperature.

Weight loss of 34% was observed between 138 and 180 °C. This correlates with the theoretical weight loss of 37% of pentafluorobenzene from **4**. Because of these encouraging results we decided to perform decomposition on preparative scale.

2.2. Synthesis of Rh(COD)(NHC)Cl

Rhodium complexes of **1a** and **1b** were prepared in good yield by application of the established silver route [14–16]

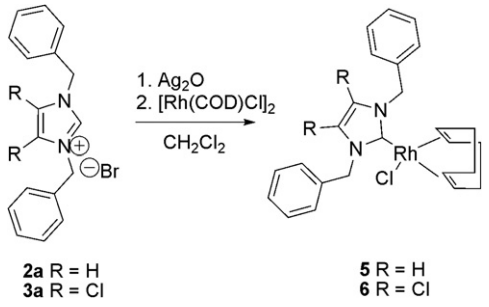

Scheme 5. Synthesis of Rh(COD)(NHC)Cl complex **5** and **6**.

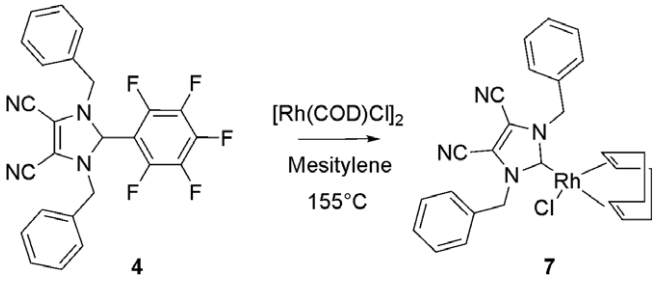

Scheme 6. Synthesis of Rh(COD)(NHC)Cl complex **7**.

Table 1
^{13}C NMR chemical shifts δ and Rh–$C_{carbene}$ coupling constants J of the carbene carbon of the complexes Rh(COD)(NHC)Cl **5**, **6**, **7** in $CDCl_3$

Complex	δ $C_{Carbene}$ [ppm]	J(Rh–$C_{Carbene}$) [Hz]
5	183.596	51.47
6	186.195	52.98
7	197.330	50.87

(Scheme 5). As mentioned above carbene **1c** could be generated by thermal decomposition of **4**. Heating the

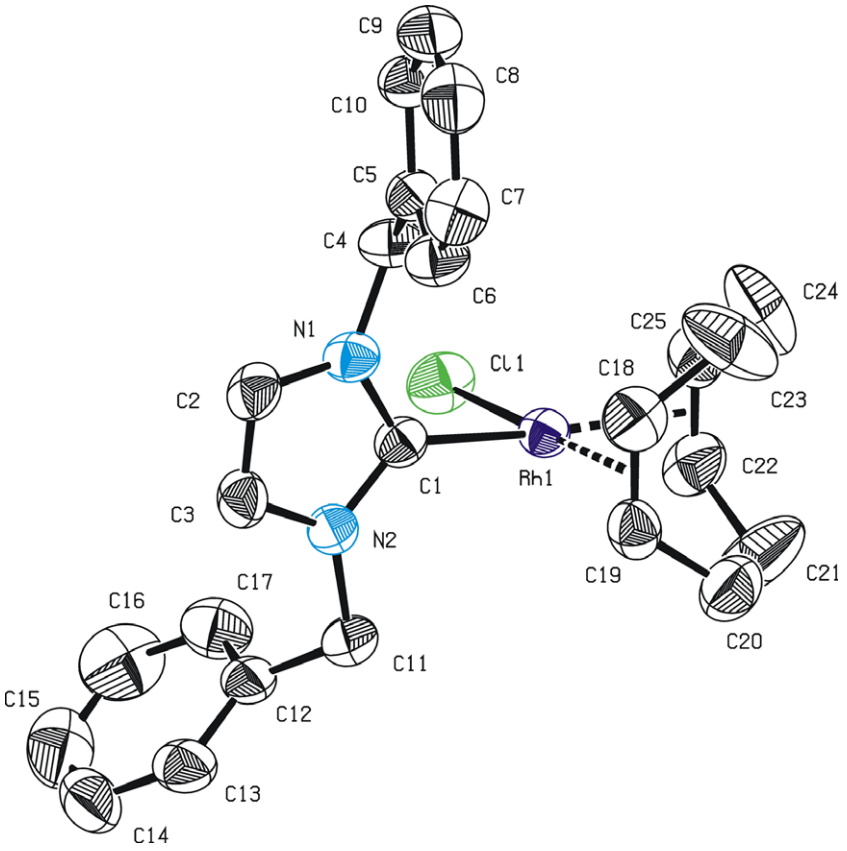

Fig. 3. ORTEP style plot of compound **5** in the solid state. Thermal ellipsoids are drawn at the 50% probability level. Hydrogen atoms are omitted for clarity.

mesitylene solution of **4** in order to achieve the generation and subsequent isolation of free carbene **1c** was not successful, showing that carbene **1c** is not stable in the free state, at least under these conditions. Performing the reaction in the presence of $[Rh(COD)Cl]_2$ under the same conditions, gave nearly quantitative yield (95%) of complex **7** (Scheme 6).

^{13}C NMR data of complexes **5**–**7** are listed in Table 1. Chemical shifts of the $Rh–C_{carbene}$ doublet are subsequently increasing from complex **5** to **7**. The corresponding resonance of **6** can be found at $\delta = 186.2$ ppm ($JC–Rh = 52.9$ Hz) and in the ^{13}C NMR spectrum of **7**, carbene C signal is at $\delta = 197.3$ ppm ($JC–Rh = 50.9$ Hz). Analogous monocarbene chloro complexes described in the literature show ^{13}C NMR carbene carbon signal at $\delta = 211.0$ ppm ($JC–Rh = 51$ Hz) for a CC-saturated NHC system, $\delta = 194.8$ ppm ($JC–Rh = 49$ Hz) for a benzimidazol-2-ylidene system and $\delta = 180.1$ ppm ($JC–Rh = 53$ Hz) for a CC-unsaturated NHC system [17]. Carbene signals of ligands **1a**–**c** can be found in the same region as benzimidazol-2-ylidene ligands, which indicates the lack of direct correlation between chemical shift and donor strength.

The chiral nature of new rhodium complexes **5**–**7** was proved by means of ^1H NMR spectroscopy where two separate doublets associated with diastereotopic hydrogens of the benzyl group could be detected. Signal of benzyl $–CH_2–$ showed no splitting even upon cooling to 193 K in our low temperature ^{13}C NMR studies of **5** and **7**. This leads to the conclusion that the conformation of these complexes cannot be frozen down to this temperature.

2.2.1. Discussion of crystal structures 5, 6 and 7

Rh(COD)(NHC)Cl complexes bearing 4,5-acceptor substituted imidazol-2-ylidene ligands are rarely studied by the means of X-ray analysis. Yellow single-crystals of **5**, **6** and **7** suitable for X-ray diffraction studies were obtained by recrystallisation from dichloromethane, acetone and acetonitrile solutions, respectively. The molecular structures of **5**, **6** and **7** are shown in Figs. 3–5. A selection of characteristic bond angles and bond distances is given in Table 2. All X-ray single-crystal diffraction studies reveal the expected square planar arrangement of the ligands at the metal centre. Complex **5** crystallized in a monoclinic crystal system in the space group $p21/n$. Compound **6** crystallized in a triclinic crystal system in the space group $P\bar{1}$ and **7** crystallized in an orthorhombic crystal system in the space group $Pna2_1$.

The Rh–carbene bond length decreases from complex **5** (2.027(2) Å) to **6** (2.015(5)/*2.017*(5) Å) to **7** (1.999(2) Å). Stronger acceptor substituents at 4,5-positions of the imidazol-2-ylidene lead to stronger π back-donation from

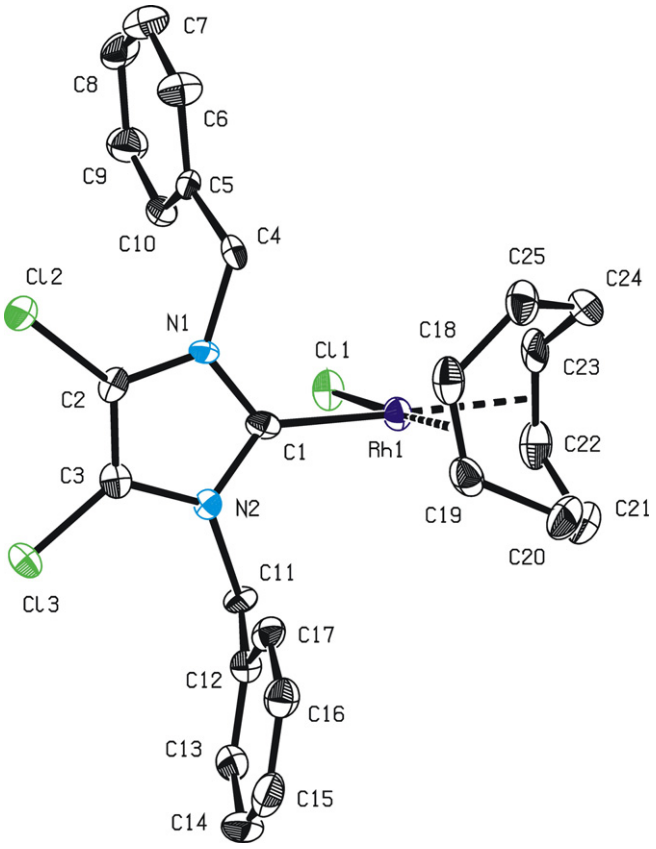

Fig. 4. ORTEP style plot of compound **6** (molecule **A**) in the solid state. Thermal ellipsoids are drawn at the 50% probability level. Hydrogen atoms are omitted for clarity.

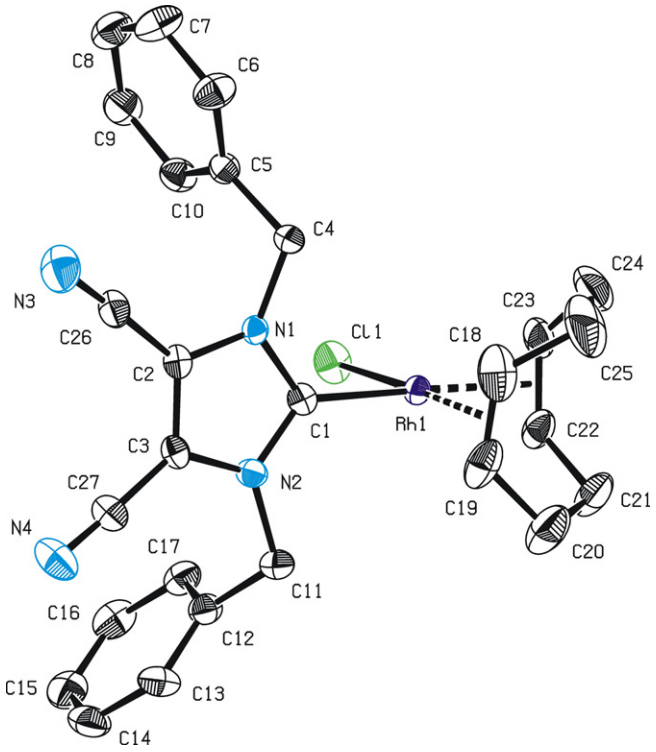

Fig. 5. ORTEP style plot of compound **7** in the solid state. Thermal ellipsoids are drawn at the 50% probability level. Hydrogen atoms are omitted for clarity.

the metal to the carbene ligand resulting in shorter rhodium–C1 bond distance. Rh–C1 bond length in **7** is the shortest one found in similar complexes in the literature. Metal–carbene distances between 2.006 and 2.036 Å have been measured by other authors for comparable systems [18,11,19].

The different *trans* influences of the carbene and chloride ligands lead to different distances between the coordinated COD carbon atoms and the Rh. As a result of the longer distance to the metal, the C22═C23 double bond *trans* to the NHC ligand is shorter than the C18═C19 bond, owing to reduced back-donation from the metal to its π^* orbital.

2.3. Synthesis and analysis of $Rh(CO)_2(NHC)Cl$

IR-spectroscopy is a valuable method allowing description of the bonding situation in metal carbonyl complexes. The CO stretching frequency is directly proportional to the back-donation from the metal centre to the CO ligand. σ-Donor ligands can therefore be compared to each other on the basis of the wavenumber of the CO stretching vibration band. A stronger σ-donor is related to a lower wavenumber of the carbon monoxide *trans* to the ligand [20].

Carbonyl substituted rhodium complexes **8**, **9**, **10** were synthesized by passing carbon monoxide at room tempera-

Table 2
Selected bond distances (Å) and angles (°) for **5**, **6** and **7**

	5	**6**[a]	**7**
Rh1–Cl1	2.3754(7)	2.3733(13)/*2.3822(13)*	2.3692(6)
Rh1–C1	2.027(2)	2.015(5)/*2.017(5)*	1.999(2)
Rh1–C18	2.116(3)	2.087(5)/*2.091(5)*	2.122(3)
Rh1–C19	2.118(2)	2.113(5)/*2.102(5)*	2.100(3)
Rh1–C22	2.214(3)	2.189(5)/*2.212(5)*	2.227(3)
Rh1–C23	2.203(3)	2.199(5)/*2.191(5)*	2.213(3)
C18–C19	1.396(4)	1.390(8)/*1.387(7)*	1.394(5)
C22–C23	1.362(4)	1.360(8)/*1.356(8)*	1.370(4)
C1–N1	1.358(3)	1.360(6)/*1.344(6)*	1.376(3)
C1–N2	1.358(3)	1.359(6)/*1.360(6)*	1.360(3)
C2–C3	1.332(3)	1.344(7)/*1.337(7)*	1.362(3)
C2–Cl2	–	1.690(5)/*1.689(5)*	–
C3–Cl3	–	1.696(5)/*1.692(5)*	–
C2–C26	–	–	1.419(3)
C3–C27	–	–	1.425(3)
C26–N3	–	–	1.140(4)
C27–N4	–	–	1.137(4)
Cl1–Rh1–C1	89.13(6)	87.80(14)/*87.90(14)*	88.64(7)
Cl1–Rh1–C18	160.63(9)	158.77(16)/*160.86(16)*	162.89(11)
Cl1–Rh1–C19	160.78(6)	162.45(16)/*160.48(15)*	158.45(10)
Cl1–Rh1–C22	91.77(7)	89.89(15)/*94.68(15)*	92.77(8)
Cl1–Rh1–C23	91.69(7)	92.83(15)/*89.67(14)*	90.34(9)
Rh1–C1–N1	125.9(2)	126.6(3)/*127.5(4)*	127.1(2)
Rh1–C1–N2	129.9(2)	129.1(4)/*127.5(4)*	128.4(2)
N1–C1–N2	104.2(2)	103.9(4)/*104.6(4)*	104.5(2)
C2–C26–N3	–	–	177.3(3)
C3–C27–N4	–	–	177.0(3)

[a] In italic the corresponding values for the second molecule **B**.

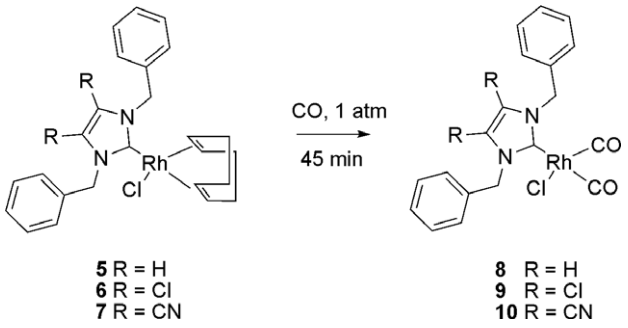

Scheme 7. Synthesis of $Rh(CO)_2(NHC)Cl$ complexes **8**–**10**.

Table 3
Carbonyl stretching frequencies ν in KBr, ^{13}C NMR chemical shifts δ and $Rh–C_{carbene}$ coupling constants J of the carbene carbon of the complexes $Rh(CO)_2(NHC)Cl$ **8**, **9**, **10** in $CDCl_3$

Complex	$\nu(CO)_{sym.}$ [cm^{-1}]	$\nu(CO)_{asym.}$ [cm^{-1}]	δ $C_{Carbene}$ [ppm]	$J(Rh–C_{Carbene})$ [Hz]
8	2074	1996	174.903	43.83
9	2084	2003	177.025	45.44
10	2088	2002	187.454	45.54

ture through a dichloromethane solution of COD substituted complexes **5**, **6**, **7** (Scheme 7). Cyclooctadiene was quantitatively displaced within minutes by carbon monoxide [18]. This reaction can be visually followed by colour change from bright to pale yellow. The CO stretching frequencies were measured in KBr and are listed in Table 3. Effects of the π-system of the NHC ligand lead to the expected result, showing that 4,5-dicyano substituted imidazol-2-ylidene has the lowest donating ability of NHC ligands in this series, because of strong acceptor substituents in the backbone. Compared with IR data for the related NHC complexes, in terms of the electronic ligand properties, these carbenes seem to range between 4,5-dihydro-imidazolin-2-ylidene ligands ($\nu(CO) = 2072$, 1999 cm^{-1}), triazol-2-ylidene ligands ($\nu(CO) = 2078$, 2006 cm^{-1}) and tetrazol-2-ylidene derivates ($\nu(CO) = 2086$, 2015 cm^{-1}) [17]. In contrast to Nolan and his group's work [21], who was performing fundamental studies on determination of electron-donating strength of various NHC ligands previously, 4,5- acceptor substituted imidazol-2-ylidene ligands show carbonyl stretching frequencies much closer to tertiary phosphine ligands than to common known NHCs [21,22].

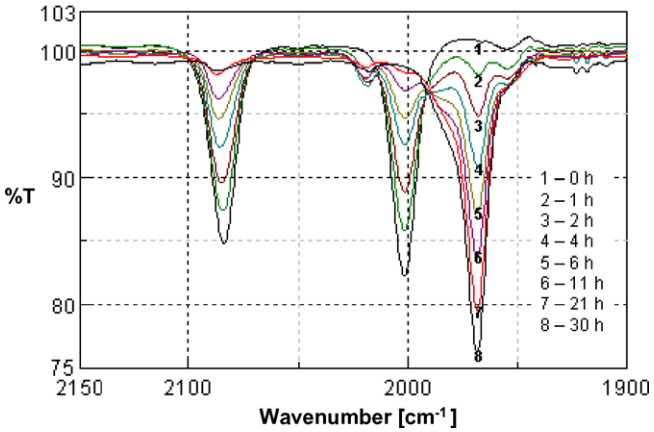

Fig. 6. IR-studies of dimerisation behaviour of **9** at 90 °C.

Strong influence of the residues R′ at N-atoms of the NHC ligands was unexpectedly found. With R′ = Me the CO stretching frequency is shifted by 10 cm^{-1} to higher wavenumbers compared to benzyl substituted ligand [11]. Because of this fact, concise conclusion about correlation of ν(CO) frequencies with the electronic properties of NHC ligands cannot be made yet.

cis-Configuration of CO ligands in these carbonyl complexes was confirmed by IR and NMR spectroscopy. IR spectra showed two strong CO stretching vibration bands of similar intensity between 2088 and 1996 cm^{-1}. Furthermore three doublets could be detected in the ^{13}C NMR spectra between $\delta = 187$ and 175 ppm, two for carbonyl and one for carbene carbons (Table 3).

All carbonyl complexes are air stable in solid state. Moreover they are soluble in polar solvents such as dichloromethane, chloroform, acetonitrile, DMSO and aromatic solvents such as toluene, but insoluble in less polar solvents such as *n*-pentane and *n*-hexane.

2.3.1. Dimerisation behaviour of $Rh(CO)_2(NHC)Cl$

During stability experiments 100% conversion of **8** to dimer **11** in dichloromethane was unexpectedly achieved. This reaction implies spontaneous loss of one molecule of

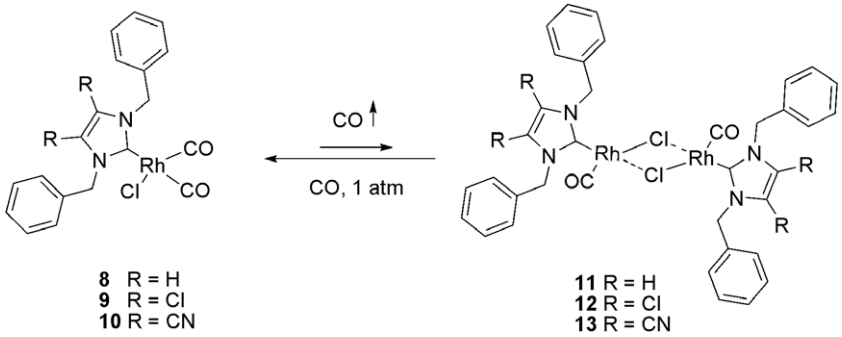

Scheme 8. Dimerisation behaviour of Rh–NHC complexes.

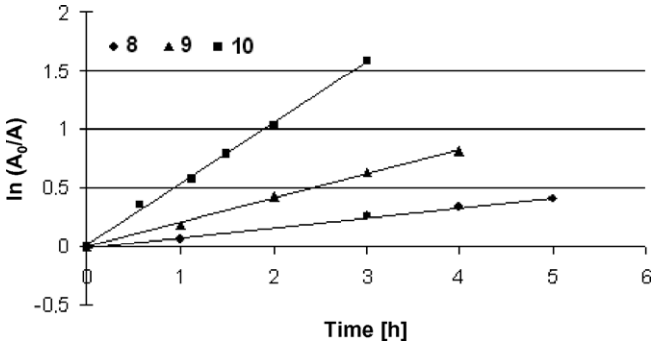

Fig. 7. Peak area vs. time. First order reaction for **8**, **9**, **10**.

Table 4
Selected bond distances and angles for **11**

Bond length (Å)		Bond angles (°)	
Rh–Cl	2.3936(6)	Cl–Rh–Cl[a]	84.92(2)
Rh–Cl[a]	2.4242(7)	Cl–Rh–C1	91.37(8)
Rh–C1	1.983(3)	Cl[a]–Rh–C1	175.09(8)
Rh–C	1.797(3)	C–Rh–C1	87.96(11)
C–O	1.152(4)	Cl–Rh–C	174.62(9)
C1–N1	1.352(3)	Cl[a]–Rh–C	96.03(9)
C1–N2	1.354(4)	Rh–C1–N1	127.7(2)
C2–C3	1.341(4)	Rh–C1–N2	127.6(2)
		N1–C1–N2	104.7(2)

[a] The symmetry operation to equivalent atom positions is $(-x, y, 0.5 - z)$.

carbon monoxide and formation of the dimer. This conversion was also repeated with complexes **8**, **9** and **10** and is shown in Scheme 8. To the best of our knowledge examples of the formation of halogeno bridged dimers are only scarcely described in the literature with the exception of elegant papers of Bielawski and Barluenga [23].

2.3.1.1. Kinetic studies. Twenty milligrams of $Rh(CO)_2$-(NHC)Cl complexes **8**, **9**, **10** were dissolved in 8 ml of toluene and stirred in an oil bath at 90 °C under Schlenk conditions while argon was bubbled through the reaction solution to achieve a complete removal of evolving CO-gas. As a result quantitative conversion to the dimers could be reached after 45 h for complex **8**, after 30 h for complex **9** and after 15 h for complex **10**. The reaction was followed by IR-spectroscopy utilizing CO vibration of the monomer at 2079 cm^{-1} for **8**, 2084 cm^{-1} for **9** and 2090 cm^{-1} for **10**, respectively, since no overlaps with the other peaks were detected. A gross estimation suggests a dimerisation on the same time scale. This means that dimerisation reaction is not the rate determining step. Fig. 6 demonstrates time dependent IR-study of monomer–dimer behaviour on the example of rhodium–NHC complex **9**. The resulting dimers showed CO peaks at 1959 cm^{-1} for **11**, 1968 cm^{-1} for **12** and 1979 cm^{-1} for **13**, respectively.

A smaller increase in dimerisation rate of complex **9** compared to **8** indicates that CO elimination from **9** is controlled by inductive effects. Higher elimination rate from **10** on the other hand can be attributed to mesomeric π-effects from cyano substituents.

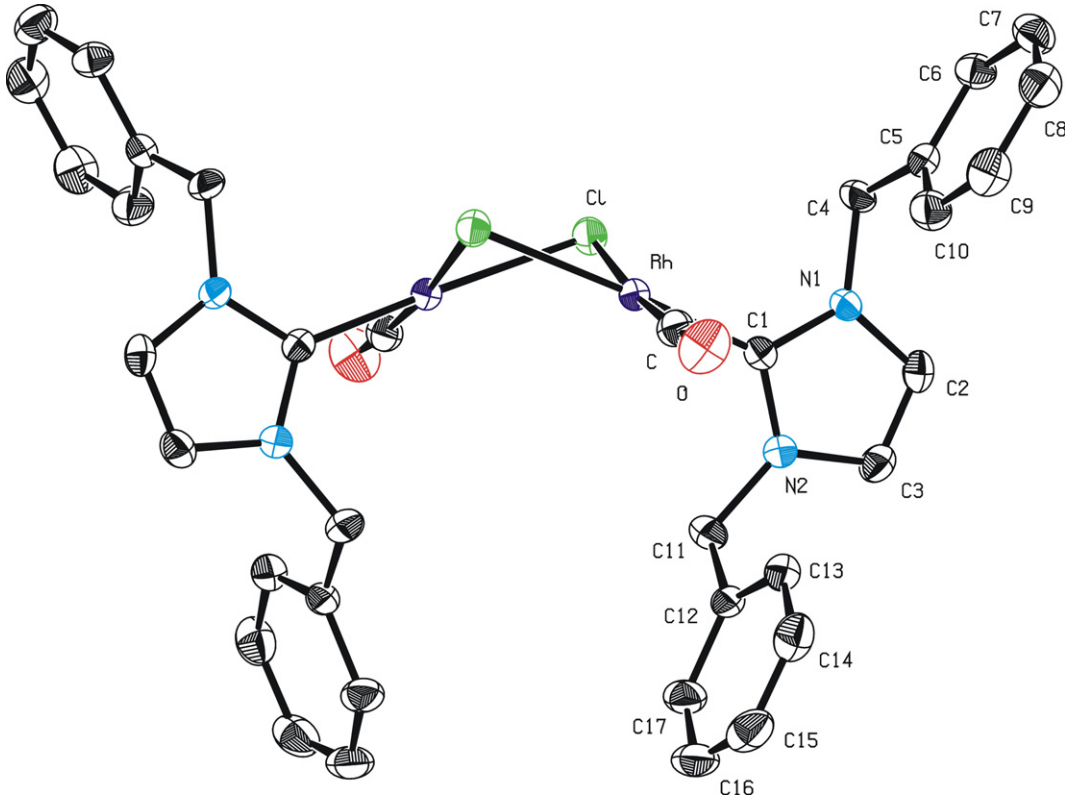

Fig. 8. ORTEP style plot of compound **11** in the solid state. Thermal ellipsoids are drawn at the 50% probability level. Symmetry operation to equivalent atom positions _*a*: $-x, y, 0.5 - z$. Hydrogen atoms are omitted for clarity.

Reaction order for the rate-determining CO-elimination step was found by plotting the peak area vs. the time, Fig. 7. First order reaction was found for complexes **8**, **9** and **10**. As a result of these measurements reaction rate coefficient was shown to increase in the series from **8** (with 0.084 s^{-1}) to **9** (with 0.207 s^{-1}) to **10** (with 0.518 s^{-1}).

Dimerisation process is completely reversible for all three complexes. The conversion back to the monomer was completed after only 15 min by passing carbon monoxide through the toluene solution of $[Rh(CO)(NHC)Cl]_2$. This reaction could be followed by the colour change from dark to pale yellow.

Reaction scheme described above is supported by these kinetic results. Since **1c** is a better π-acceptor ligand, higher CO-elimination rate is favoured due to M–CO bond destabilisation.

2.4. Discussion of crystal structures *11*

Crystal structure of **11** (Fig. 8) consists of discrete dinuclear units of the formula $[Rh(CO)(C_{17}H_{16}N_2)Cl]_2$. A selection of characteristic bond angles and bond distances is given in Table 4. The complex crystallized out of dichloromethane in a monoclinic crystal system in the space group *C*2/*c*. The bonding distance between Rh and C1 is 1.983(3) Å. The Rh–Cl distance averages 2.409 Å. The coordination around each rhodium atom is square-planar. The dihedral angle between the two square planes of 55.92° gives a bent configuration of the molecule in which the CO and the carbene ligands are in a *cis* arrangement. Dimers similar to our system are only rarely known. By the comparison of data presented in this paper with the results of Bielawski et al. similarities in the crystal system and bonding distances for $[Rh(CO)(NHC)Cl]_2$ can be found [23].

3. Conclusion

New types of 4,5-acceptor substituted NHC ligands have been synthesized. Neutral rhodium complexes were obtained either via *in situ* transmetalation from silver complexes or via thermal decomposition of pentafluorobenzene adducts. Introduction of acceptor substituents such as chloro- or cyano-groups at the 4,5-positions of imidazol-2-ylidene reduces donor strength of the ligands either due inductive (Cl) or π-acceptor (CN) effects. This was supported by dimerisation behaviour analysis of NHC–rhodium carbonyl complexes. Theoretical studies of these effects are currently on investigation. Since *N*-substitution has a strong influence on the electronic properties, NHC ligands will be further modified in our laboratory. We shall report on this in due time soon.

4. Experimental

4.1. General

1,3-Diphenylimidazolium salt, *N*,*N*′-dibenzyldiaminomaleonitrile were prepared according to literature procedures [13,24]. All other starting materials were obtained commercially and were used as received. All syntheses, except as noted, were performed under an atmosphere of argon, using solvents dried on an alumina-based solvent purification system. Mesitylene was dried over $LiAlH_4$. ^1H and ^{13}C NMR spectra were recorded on a JEOL JMX-GX 400 MHz spectrometer at room temperature and referenced to the residual ^1H and ^{13}C signals of the solvents. Chemical shifts are given in ppm. NMR multiplicities are abbreviated as follows: s = singlet, d = doublet, t = triplet, q = quartet, p = quintet, sept = septet, m = multiplet, br = broad signal. MS spectra were measured at the TU München Mass Spectrometry Laboratory on a Finnigan MAT 90 mass spectrometer using the CI or FAB technique. IR spectra were acquired using a Jasco FT/IR-460 Plus spectrometer. Thermogravimetric mass spectra (TGA) analysis measurements were conducted with a Netzsch TG209 system; typically about 10 mg of each sample was heated from 35 to 700 °C at 10 K min^{-1}. Elemental analyses were carried out by the Microanalytical Laboratory at the TU München. Melting points were measured with a Büchi melting point apparatus system (Dr. Tottoli).

4.2. 4,5-Dichloro-1-benzylimidazole *3*

4,5-Dichloro-1*H*-imidazole (0.80 g, 5.84 mmol) and K_2CO_3 (1.21 g, 8.76 mmol) were stirred for 10 min in 30 ml of acetonitrile. Benzyl bromide (0.69 ml, 5.84 mmol) was added in one portion and stirring was continued at room temperature for further 2 days. After the solvent was removed under reduced pressure 70 ml of water were added. The aqueous phase was extracted with CH_2Cl_2 (4 × 20 ml). Organic phases were combined and dried over sodium sulphate. **3** was obtained as orange solid after solvent removal under reduced pressure (1.24 g, 93%).

Mp: 50–51 °C. ^1H NMR ($CDCl_3$): $\delta = 7.32$ (s, 1H, NCHN), 7.24 (m, 3H, C_{benzyl}), 7.08 (m, 2H, C_{benzyl}), 4.95 (s, 2H, CH_2). ^{13}C NMR ($CDCl_3$): $\delta = 134.32$ (NCHN), 134.15, 128.71, 128.17, 127.06 (C_{benzyl}), 125.80, 113.15 (CCl), 49.34 (CH_2). IR (KBr): $\nu_{max}/cm^{-1} = 3122$ (C–Cl), 1520, 1496, 1483, 1455, 1437, 1388, 1346, 1254, 1180, 1115, 976, 808, 721, 694, 663, 638, 503. MS (CI): *m*/*z* 227.1 (100%, $M+H^+$), 226.1 (4%, M^+).

4.3. 4,5-Dichloro-1,3-dibenzylimidazoliumbromide *3a*

Benzyl bromide (0.79 ml, 6.61 mmol) was added in one portion to a stirred suspension of 4,5-dichloro-1-benzylimidazole (0.50 g, 2.20 mmol) in 5 ml of toluene. The mixture was stirred for 40 h at room temperature. Afterwards the solvent was removed under reduced pressure. The residue was washed with THF (4 × 5 ml) and the title compound was isolated as a white solid (609 mg, 69%).

Mp: 177–178 °C. ^1H NMR ($CDCl_3$): $\delta = 11.78$ (s, 1H, NCHN), 7.54 (m, 4H, C_{benzyl}), 7.32 (m, 6H, C_{benzyl}), 5.63 (s, 4H, CH_2). ^{13}C NMR ($CDCl_3$): $\delta = 138.03$ (NCHN),

131.73, 129.61, 129.47, 128.99 (C_{benzyl}), 119.36 (CCl), 52.83 (CH_2). IR (KBr): $\nu_{max}/cm^{-1} = 3098$, 3012, 2861 (C–Cl), 1586, 1550, 1498, 1456, 1405, 1363, 1343, 1304, 1205, 1181, 1146, 1078, 1032, 769, 731, 709, 697, 607. Anal. Calc. for $C_{17}H_{15}Cl_2N_2Br$ (398.12): C, 51.3; H, 3.8; N, 7.0; Cl, 17.8. Found: C, 51.24; H, 3.72; N, 7.05; Cl, 18.21%. MS (FAB): *m/z* 319.1 (67%, M^+-Br), 317.1 (100%, $M^+-Br-2H$).

4.4. 4,5-Dicyano-1,3-dibenzyl-2-(pentafluorophenyl)-2,3-dihydro-imidazole **4**

In a 5 ml vial equipped with a magnetic stirrer bar pentafluorobenzaldehyde (1.36 g, 6.94 mmol) was dissolved in 1 ml of acetic acid. *N*,*N*′-Dibenzyldiaminomaleonitrile (1.00 g, 3.47 mmol) was added in one portion and the reaction mixture was stirred at room temperature for 2 days. The brown precipitate was filtered off and washed once with 5 ml of water and three times with 3 ml of cold methanol. Compound **4** was obtained as a light yellow solid after drying under reduced pressure (1.317 g, 81%).

Mp: 155 °C (decomp.). ^{1}H NMR ($CDCl_3$): $\delta = 7.22$ (br, 6H, C_{benzyl}), 7.04 (br, 4H, C_{benzyl}), 5.79 (s, 1H, NCHN), 4.09 (d, 2H, ^2J(H–C–H) = 14.8 Hz, $CH_{2benzyl}$), 3.94 (d, 2H, ^2J(H–C–H) = 14.4 Hz, $CH_{2benzyl}$). ^{13}C NMR ($CDCl_3$): $\delta = 146.50$, 143.98, 140.49, 138.49, 136.00 (m, CF), 133.22, 128.85, 128.76 (C_{benzyl}), 113.88 (CCN), 112.40 (m, CCF), 110.61 (NCCN), 77.66 (NCHN), 54.19 (CH2). IR (KBr): $\nu_{max}/cm^{-1} = 2215$ (CN), 1655, 1592, 1522, 1511, 1456, 1383, 1359, 1209, 1188, 1150, 1002, 921, 747, 703, 693. Anal. Calc. for $C_{25}H_{15}F_5N_4$ (466.41): C, 64.4; H, 3.24; N, 12.0. Found: C, 64.5; H, 3.10; N, 11.6%. MS (FAB): *m/z* 467.1 (52%, $M+H^+$), 466.1 (100%, M^+).

4.5. General procedure for the preparation of NHC complexes **5** and **6**

To the solution of imidazolium salt (2 equiv.) in CH_2Cl_2 (20 ml) silver(I) oxide (1 equiv.) was added in one portion. Resulting suspension was stirred for 3 h in the darkness, during which time the black colour gradually diminished. The reaction mixture was filtered through a small pad of Celite and 1 equiv. of $[Rh(COD)Cl]_2$ was added in one portion. Almost immediately a white precipitate of silver salt was formed. The reaction mixture was stirred for additional 18 h. The solvent was evaporated and the residue was purified by flash chromatography on silica gel with CH_2Cl_2 as eluent.

4.5.1. Chloro(η^4-1,5-COD)(1,3-dibenzylimidazol-2-yliden)rhodium(I) **5**

Two hundred milligrams (0.607 mmol) of **2a**, 70 mg (0.304 mmol) of silver(I) oxide and 150 mg (0.304 mmol) of $[Rh(COD)Cl]_2$ yielded **5** as a yellow solid (150 mg, 100%).

Mp: 208 °C (decomp.). ^{1}H NMR ($CDCl_3$): $\delta = 7.38$ (m, 10H, CH_{benzyl}), 6.65 (s, 2H, $CH_{imidazol}$), 5.88 (d, 2H, ^2J(H–C–H) = 14.8 Hz, $CH_{2benzyl}$), 5.76 (d, 2H, ^2J(H–C–H) = 14.8 Hz, $CH_{2benzyl}$), 5.07 (m, 2H, cod_{vinyl}), 3.32 (m, 2H, cod_{vinyl}), 2.31 (m, 4H, cod_{allyl}), 1.88 (m, 4H, cod_{allyl}). ^{13}C NMR ($CDCl_3$): $\delta = 183.60$ (d, ^1J(C–Rh) = 51.5 Hz, NCN), 136.54, 128.96, 128.26, 128.18, (C_{benzyl}), 120.98 ($C_{imidazol}$), 98.90, 98.83, 68.49, 68.35 (cod_{vinyl}), 54.69 ($CH_{2benzyl}$), 32.94, 28.85 (cod_{allyl}). IR (KBr): $\nu_{max}/cm^{-1} = 2933$, 2905, 2873, 2832, 1637, 1619, 1496, 1453, 1416, 1398, 1361, 1223, 1078, 1029, 960, 766, 727, 715, 699. MS (FAB): *m/z* 494.1 (4%, M^+), 459.1 (21%, M^+-Cl), 386.0 (38%, M^+-COD), 351.1 (100%, $M^+-Cl-COD$).

4.5.2. Chloro(η^4-1,5-COD)(4,5-dichloro-1,3-dibenzylimidazol-2-yliden)rhodium(I) **6**

Two hundred milligrams (0.502 mmol) of **3a**, 58 mg (0.251 mmol) of silver(I) oxide and 124 mg (0.251 mmol) of $[Rh(COD)Cl]_2$ yielded **6** as of a yellow solid (142 mg, 100%).

Mp: 214 °C (decomp.). ^{1}H NMR ($CDCl_3$): $\delta = 7.37$ (m, 10H, CH_{benzyl}), 6.04 (d, 2H, ^2J(H–C–H) = 15.6 Hz, $CH_{2benzyl}$), 5.89 (d, 2H, ^2J(H–C–H) = 15.6 Hz, $CH_{2benzyl}$), 5.06 (m, 2H, cod_{vinyl}), 3.07 (m, 2H, cod_{vinyl}), 2.24 (m, 2H, cod_{allyl}), 2.01 (m, 2H, cod_{allyl}), 1.82 (m, 2H, cod_{allyl}), 1.68 (m, 2H, cod_{allyl}). ^{13}C NMR ($CDCl_3$): $\delta = 186.20$ (d, ^1J(C–Rh) = 53.0 Hz, NCN), 135.82, 128.90, 128.01, 127.07 (C_{benzyl}), 117.20 (CCl), 99.71, 99.64, 69.81, 69.67 (cod_{vinyl}), 54.00 ($CH_{2benzyl}$), 32.66, 28.67 (cod_{allyl}). IR (KBr): $\nu_{max}/cm^{-1} = 2934$, 2914, 2878 (C–Cl), 2830 (C–Cl), 1637, 1618, 1592, 1495, 1454, 1429, 1389, 1350, 1329, 1216, 968, 722, 692. Anal. Calc. for $C_{25}H_{26}Cl_3N_2Rh$ (563.75): C, 53.3; H, 4.6; N, 4.97. Found: C, 53.96; H, 4.83; N, 4.81%. MS (FAB): *m/z* 562.0 (8%, M^+), 527.1 (44%, M^+-Cl), 419.0 (100%, $M^+-Cl-COD$).

4.6. Chloro(η^4-1,5-COD)(4,5-dicyano-1,3-dibenzylimidazol-2-yliden)rhodium(I) **7**

Ninety-seven milligrams (0.208 mmol) of **4** were dissolved in 6 ml of dry mesitylene. 51 mg (0.104 mmol) of $[Rh(COD)Cl]_2$ were added in one portion and the mixture was heated to 165 °C. After 16 h the solvent was evaporated and the residue was purified by flash chromatography on silica gel with CH_2Cl_2 as eluent. Recrystallisation out of 1-propanole yielded **7** (54 mg, 95%) as a yellow solid.

Mp: 132 °C (decomp.). ^{1}H NMR ($CDCl_3$): $\delta = 7.47$ (m, 10H, CH_{benzyl}), 6.26 (d, 2H, ^2J(H–C–H) = 15.2 Hz, $CH_{2benzyl}$), 5.89 (d, ^{2}H, ^2J(H–C–H) = 15.2 Hz, $CH_{2benzyl}$), 5.24 (m, 2H, cod_{vinyl}), 3.16 (m, 2H, cod_{vinyl}), 2.35 (m, 2H, cod_{allyl}), 2.22 (m, 2H, cod_{allyl}), 1.92 (m, 4H, cod_{allyl}). ^{13}C NMR ($CDCl_3$): $\delta = 197.33$ (d, ^1J(C–Rh) = 50.9 Hz, NCN), 133.54, 129.38, 128.44 (C_{benzyl}), 115.76 (CN), 106.43 (CCN), 102.32, 102.25, 70.66, 70.52 (cod_{vinyl}), 55.88 ($CH_{2benzyl}$), 32.73, 28.68 (cod_{allyl}). IR (KBr): $\nu_{max}/cm^{-1} = 2938$, 2914, 2882, 2830, 2360, 2342, 2238 (CN), 1637, 1617,1497, 1459, 1440, 1400, 1332, 1214, 735, 697. Anal. Calc. for $C_{27}H_{26}ClN_4Rh$ (544.85): C, 59.5; H, 4.81;

N 10.3. Found: C, 59.4; H, 5.21; N, 9.82%. MS (FAB): *m/z* 544.0 (18%, M^+), 509.1 (57%, M^+-Cl), 436.0 (39% M^+-COD), 401.0 (100%, $M^+-Cl-COD$).

4.7. General procedure for the preparation of dicarbonyl complexes

Carbon monoxide was bubbled for 45 min through a solution of NHC rhodium complex in CH_2Cl_2. After the colour had changed to pale yellow, the solvent was removed *in vacuo* and the crude product was washed with *n*-pentane (2 × 5 ml).

4.7.1. Chloro-dicarbonyl(1,3-dibenzylimidazol-2-yliden)rhodium(I) 8

Two hundred and fifty milligrams (0.505 mmol) of **5** yielded **8** as a light yellow solid (207 mg, 95%). Mp: 211 °C (decomp.). ^{1}H NMR ($CDCl_3$): $\delta = 7.36$ (m, 10H, CH_{benzyl}), 6.85 (s, 2H, $CH_{imidazol}$), 5.56 (d, 2H, ^2J(H–C–H) = 14.0 Hz, $CH_{2benzyl}$), 5.47 (d, 2H, ^2J(H–C–H) = 14.4 Hz, $CH_{2benzyl}$). ^{13}C NMR ($CDCl_3$): $\delta = 185.44$ (d, ^1J(C–Rh) = 54.1 Hz, CO), 182.34 (d, ^1J(C–Rh) = 74.3 Hz, CO), 174.90 (d, ^1J(C–Rh) = 43.8 Hz, NCN), 135.54, 129.01, 128.54, 128.32 (C_{benzyl}), 121.91 ($C_{imidazol}$), 55.10 ($CH_{2benzyl}$). IR (KBr): $\nu_{max}/cm^{-1} = 2074$ (CO), 1996 (CO), 1637, 1605, 1564, 1496, 1452, 1416, 1358, 1236, 1173, 763, 744, 727, 713, 693, 584. Anal. Calc. for $C_{19}H_{16}ClN_2O_2Rh$ (442.70): C, 51.54; H, 3.64; N. 6.32. Found: C, 51.64; H, 3.74; N, 6.25%. MS (FAB): *m/z* 442.0 (4%, M^+), 386.0 (53%, M^+-2CO), 351.1 (100%, $M^+-2CO-Cl$).

4.7.2. Chloro-dicarbonyl(4,5-dichloro-1,3-dibenzylimidazol-2-yliden)rhodium(I) 9

One hundred and fifty milligrams (0.266 mmol) of **6** yielded **9** as a light yellow solid (125 mg, 92%). Mp: 222 °C (decomp.). ^{1}H NMR ($CDCl_3$): $\delta = 7.38$ (m, 10H, CH_{benzyl}), 5.77 (d, 2H, ^2J(H–C–H) = 15.2 Hz, $CH_{2benzyl}$), 5.53 (d, 2H, ^2J(H–C–H) = 15.6 Hz, $CH_{2benzyl}$). ^{13}C NMR ($CDCl_3$): $\delta = 184.78$ (d, ^1J(C–Rh) = 55.1 Hz, CO), 181.41 (d, ^1J(C–Rh) = 73.7 Hz, CO), 177.03 (d, ^1J(C–Rh) = 45.4 Hz, NCN), 134.38, 128.95, 128.55, 127.64 (C_{benzyl}), 118.34, 118.32 (CCl), 54.03 ($CH_{2benzyl}$). IR (KBr): $\nu_{max}/cm^{-1} = 2084$ (CO), 2003 (CO), 1637, 1619, 1590, 1496, 1456, 1438, 1399, 1350, 1211, 725, 693, 584. Anal. Calc. for $C_{19}H_{14}Cl_3N_2O_2Rh$ (511.59): C, 44.6; H, 2.76; N, 5.48. Found: C, 44.67; H, 2.89; N, 5.46%. MS (FAB): *m/z* 509.9 (5%, M^+), 453.9 (49%, M^+-2CO), 418.9 (100%, $M^+-2CO-Cl$).

4.7.3. Chloro-dicarbonyl(4,5-dicyano-1,3-dibenzylimidazol-2-yliden)rhodium(I) 10

One hundred and eighteen milligrams (0.217 mmol) of **7** yielded **10** as a light yellow solid (107 mg, 100%). Mp: 158 °C (decomp.). ^{1}H NMR ($CDCl_3$): $\delta = 7.46$ (m, 10H, CH_{benzyl}), 5.83 (d, 2H, ^2J(H–C–H) = 14.8 Hz, $CH_{2benzyl}$), 5.70 (d, 2H, ^2J(H–C–H) = 15.2 Hz, $CH_{2benzyl}$). ^{13}C NMR ($CDCl_3$): $\delta = 187.45$ (d, ^1J(C–Rh) = 45.5 Hz, NCN), 184.05 (d, ^1J(C–Rh) = 55.6 Hz, CO), 180.93 (d, ^1J(C–Rh) = 72.6 Hz, CO), 132.60, 129.91, 129.53, 128.86 (C_{benzyl}), 116.08 (CCN), 106.13 (CN), 56.42 ($CH_{2benzyl}$). IR (KBr): $\nu_{max}/cm^{-1} = 2241$ (CN), 2088 (CO), 2002 (CO), 1974, 1624, 1605, 1497, 1460, 1443, 1401, 1344, 1205, 743, 697. Anal. Calc. for $C_{21}H_{14}ClN_4O_2Rh$ (492.73): C, 51.20; H, 2.86; N, 11.40. Found: C, 52.10; H, 3.32; N, 11.60%. MS (FAB): *m/z* 492.0 (3%, M^+), 436.1 (44%, M^+-2CO), 401.1 (100%, $M^+-2CO-Cl$).

4.8. Single-crystal X-ray structure determination of compounds 5, 6, 7, and 11

4.8.1. General

Crystal data and details of the structure determination are presented in Table 5. Suitable single-crystals for the X-ray diffraction study were grown with standard cooling techniques. Crystals were stored under perfluorinated ether, transferred in a Lindemann capillary, fixed, and sealed. Preliminary examination and data collection were carried out on an area detecting system and graphite-monochromated Mo Kα radiation ($\lambda = 0.71073$ Å). The unit cell parameters were obtained by full-matrix least-squares refinements during the scaling procedure. Data collections for **6**, **7**, and **11** were performed at low temperatures (Oxford Cryosystems cooling device). Each crystal was measured with a couple of data sets in rotation scan modus. Intensities were integrated and the raw data were corrected for Lorentz, polarization, and, arising from the scaling procedure for latent decay and absorption effects. The structures were solved by a combination of direct methods and difference Fourier syntheses. All non-hydrogen atoms were refined with anisotropic displacement parameters. All hydrogen atoms were placed in ideal positions and refined using a riding model, with methylene and aromatic d_{C-H} distances of (1.00, 0.99 or 0.97 Å) and (0.95 or 0.93 Å), respectively, and $U_{iso(H)} = 1.2U_{eq(C)}$. Full-matrix least-squares refinements were carried out by minimizing $\sum w(F_o^2 - F_c^2)^2$ with the SHELXL-97 weighting scheme and stopped at shift/err <0.001. The final residual electron density maps showed no remarkable features. Neutral atom scattering factors for all atoms and anomalous dispersion corrections for the non-hydrogen atoms were taken from International Tables for Crystallography. All calculations were performed with the WINGX system, including the programs PLATON, SHELXL-97, and SIR92 [25]. Specials: Compound **5**: (Stoe & Cie. GmbH, IPDS 2T; rotating anode, Nonius FR591; two data sets in rotation scan modus with $\Delta\omega = 1.00°$; d$x = 120$; $T = 293$ K). Compound **6**: (Oxford Diffraction, XCALIBUR, κ-CCD; sealed tube, Enhance X-ray Source, Spellman, DF3; five data sets in rotation scan modus with $\Delta\phi/\Delta\omega = 2.00°$; d$x = 50$; $T = 150$ K). The low scattering power of the very tiny crystal forced us to cut the data set at $\theta = 23.36°$. The asymmetric unit contains two crystallographic independent molecules **A** and **B** of the target compound **6**. Compound

Table 5
Crystallographic data for compounds **5**, **6**, **7**, and **11**

	5	**6**	**7**	**11**
Formula	$C_{25}H_{28}ClN_2Rh$	$C_{25}H_{26}Cl_3N_2Rh$	$C_{27}H_{26}ClN_4Rh$	$C_{36}H_{32}Cl_2N_4O_2Rh_2$
Fw	494.85	563.74	544.88	829.38
Colour/habit	Yellow/prism	Yellow/fragment	Yellow/fragment	Orange/needle
Crystal dimensions (mm)	0.18 × 0.20 × 0.53	0.02 × 0.08 × 0.10	0.20 × 0.30 × 0.40	0.05 × 0.25 × 1.02
Crystal system	Monoclinic	Triclinic	Orthorhombic	Monoclinic
Space group	$P2_1/n$ (no. 14)	$P\bar{1}$ (no. 2)	$Pna2_1$ (no. 33)	$C2/c$ (no. 15)
a (Å)	12.1509(5)	6.6565(4)	13.8499(1)	25.1555(3)
b (Å)	10.8551(6)	14.765(1)	17.8600(1)	9.7908(1)
c (Å)	17.2545(7)	24.472(2)	9.7770(1)	13.5338(2)
α (°)	90	98.875(6)	90	90
β (°)	101.815(3)	94.681(5)	90	95.387(1)
γ (°)	90	98.282(5)	90	90
V (Å^3)	2227.64(18)	2338.3(3)	2418.43(3)	3318.55(7)
Z	4	4	4	4
T (K)	293	150	150	153
D_{calc} (g cm^{-3})	1.475	1.601	1.497	1.660
μ (mm^{-1})	0.900	1.089	0.839	1.195
$F(000)$	1016	1144	1112	1664
θ Range (°)	3.88–25.25	3.04–23.36	2.79–27.85	2.74–25.35
Index ranges (h,k,l)	±14, ±13, ±20	±7, ±16, ±27	±18, ±23, ±12	±30, ±11, ±16
Number of reflections collected	27660	23652	54826	29441
Number of independent reflections/R_{int}	4016/0.033	6768/0.045	5756/0.016	3029/0.019
Number of observed reflections [$I_o > 2\sigma(I_o)$]	3372	4797	5496	2726
Number of data/restraints/parameters	4016/0/262	6768/0/559	5756/1/298	3029/0/208
R_1/wR_2 [$I_o > 2\sigma(I_o)$][a]	0.0230/0.0579	0.0365/0.0681	0.0234/0.0553	0.0240/0.0554
R_1/wR_2 (all data)[a]	0.0297/0.0591	0.0609/0.0797	0.0255/0.0578	0.0293/0.0608
GOF (on F^2)[a]	0.978	1.095	1.127	1.212
Largest difference in peak and hole (e Å^{-3})	+0.32/−0.38	+0.57/−0.45	+0.60/−0.55	+0.43/−0.62

[a] $R_1 = \sum(||F_o| - |F_c||)/\Sigma|F_o|$; $wR_2 = \{\sum[w(F_o^2 - F_c^2)^2]/\sum[w(F_o^2)^2]\}^{1/2}$; GOF $= \{\sum[w(F_o^2 - F_c^2)^2]/(n-p)\}^{1/2}$.

7: (Oxford Diffraction, XCALIBUR, κ-CCD; sealed tube, Enhance X-ray Source, Spellman, DF3; nine data sets in rotation scan modus with $\Delta\phi/\Delta\omega = 1.00°$; d$x = 50$; $T = 150$ K). The correct enantiomer is proved by Flack's parameter $\varepsilon = 0.03(2)$. Compound **11**: (Oxford Diffraction, XCALIBUR, κ-CCD; sealed tube, Enhance X-ray Source, Spellman, DF3; nine data sets in rotation scan modus with $\Delta\phi/\Delta\omega = 1.00°$; d$x = 50$; $T = 153$ K).

Acknowledgement

We gratefully acknowledge financial support from the BMBF (Bundesministerium für Bildung und Forschung).

Appendix A. Supplementary material

CCDC 676401, 676402, 676403 and 676404 contain the supplementary crystallographic data for **5**, **6**, **7**, and **11**. These data can be obtained free of charge from The Cambridge Crystallographic Data Centre via www.ccdc.cam.ac.uk/data_request/cif. Supplementary data associated with this article can be found, in the online version, at doi:10.1016/j.jorganchem.2008.01.039.

References

[1] K.J. Öfele, J. Organomet. Chem. 12 (1968) P42.
[2] H.W. Wanzlick, H.J. Schönherr, Angew. Chem., Int. Ed. 7 (1968) 141.
[3] (a) A.J. Arduengo III, R.L. Harlow, M. Kline, J. Am. Chem. Soc. 113 (1991) 361;
(b) A.J. Arduengo III, H.V.R. Dias, R.L. Harlow, M. Kline, J. Am. Chem. Soc. 114 (1992) 5530.
[4] (a) W.A. Herrmann, C. Köcher, Angew. Chem., Int. Ed. 36 (1997) 2162;
(b) E.A.B. Kantchev, C.J. O'Brian, M.G. Organ, Angew. Chem., Int. Ed. 46 (2007) 2768;
(c) T. Weskamp, V.P.W. Böhm, W.A. Herrmann, J. Organomet. Chem. 600 (2000) 12.
[5] (a) W.A. Herrman, Angew. Chem., Int. Ed. 41 (2002) 1290;
(b) S.P. Nolan (Ed.), *N*-Heterocyclic Carbenes in Synthesis, Wiley-VCH, 2006, ISBN 3-527-31400-8.
[6] S.K. Schneider, P. Roembke, G.R. Julius, C. Loschen, H.G. Raubenheimer, G. Frenking, W.A. Herrmann, Eur. J. Inorg. Chem. 15 (2005) 2973.
[7] (a) Q. Yao, M. Zabawa, J. Woo, C. Zheng, J. Am. Chem. Soc. 129 (2007) 3088;
(b) S.G. Fiddy, J. Evans, T. Neisius, M.A. Newton, N. Tsoureas, A.A.D. Tulloch, A.A. Danopoulos, Chem. Eur. J. 13 (2007) 3652;
(c) M.-T. Lee, H.M. Lee, C.-H. Hu, Organometallics 26 (2007) 1317;
(d) K. Hara, Y. Kanamori, M. Sawamura, Bull. Chem. Soc. Jpn. 79 (2006) 1781.
[8] V. Lavallo, Y. Canac, B. Donnadieu, W.W. Schoeller, G. Bertrand, Angew. Chem. 118 (2006) 3568.
[9] G.D. Frey, V. Lavallo, B. Donnadieu, W.W. Schoeller, G. Bertrand, Science 316 (2007) 439.
[10] (a) M. Viciano, E. Mas-Marzá, M. Sanaú, E. Peris, Organometallics 25 (2006) 3063;
(b) R. Corberán, J. Ramírez, M. Poyatos, E. Peris, E. Fernández, Tetrahedron: Asymmetry 17 (2006) 1759;

(c) V. Lillo, J. Mata, J. Ramírez, E. Peris, E. Fernandez, Organometallics 25 (2006) 5829;
(d) C. Vicent, M. Viciano, E. Mas-Marzá, M. Sanaú, E. Peris, Organometallics 25 (2006) 3713;
(e) R. Corberán, M. Sanaú, E. Peris, J. Am. Chem. Soc. 128 (2006) 3974.
[11] D.M. Khramov, V.M. Lynch, C.W. Bielawski, Organometallics 26 (2007) 6042.
[12] (a) G.W. Nyce, S. Csihony, R.M. Waymouth, J.L. Hedrick, Chem. Eur. J. 10 (2004) 4073;
(b) A.P. Blum, T. Ritter, R.H. Grubbs, Organometallics 26 (2007) 2122.
[13] R.W. Begland, D.R. Hartter, F.N. Jones, D.J. Sam, W.A. Sheppard, O.W. Webster, F.J. Weigert, J. Org. Chem. 39 (1974) 2341.
[14] H.M.J. Wang, I.J.B. Lin, Organometallics 17 (1998) 972.
[15] (a) A.R. Chianese, X. Li, M.C. Janzen, J.W. Faller, R.H. Crabtree, Organometallics 22 (2003) 1663;
(b) B. Bildstein, M. Malaun, H. Kopacka, K. Wurst, M. Mitterböck, K.H. Ongania, G. Opromolla, P. Zanello, Organometallics 18 (1999) 4325;
(c) C.K. Lee, K.M. Lee, I.J.B. Lin, Organometallics 21 (2002) 10;
(d) K.M. Lee, H.M.J. Wang, I.J.B. Lin, J. Chem. Soc., Dalton Trans. (2002) 2852.
[16] (a) D. Baskakov, W.A. Herrmann, E. Herdtweck, S.D. Hoffmann, Organometallics 26 (2007) 626;
(b) A. Kascatan-Nebioglu, M.J. Panter, J.C. Garrison, C.A. Tessier, W.J. Youngs, Organometallics 23 (2004) 1928.
[17] W.A. Herrmann, J. Schütz, G.D. Frey, E. Herdtweck, Organometallics 25 (2006) 2437.
[18] W.A. Herrmann, M. Elison, F. Fischer, C. Köcher, G.R.J. Artus, Chem. Eur. J. 2 (1996) 772.
[19] (a) K.H. Park, S.Y. Kim, S.U. Son, Y.K. Chung, Eur. J. Org. Chem. (2003) 4341;
(b) H. Seo, B.Y. Kim, J.H. Lee, H.J. Park, S.U. Son, Y.K. Chung, Organometallics 22 (2003) 4783;
(c) M.V. Baker, S.K. Brayshaw, B.W. Skelton, A.H. White, Inorg. Chim. Acta 357 (2004) 2841;
(d) S. Saravanakumar, A.I. Oprea, M.K. Kindermann, P.G. Jones, J. Heinicke, Chem. Eur. J. 12 (2006) 3143.
[20] K. Denk, P. Sirsch, W.A. Herrmann, J. Organomet. Chem. 649 (2002) 219.
[21] R.A. Kelly, H. Clavier, S. Giudice, N.M. Scott, E.D. Stevens, J. Bordner, I. Samardjiev, C.D. Hoff, L. Cavallo, S.P. Nolan, Organometallics 27 (2008) 202.
[22] (a) W.A. Herrmann, D. Baskakov, E. Herdtweck, S.D. Hoffmann, T. Bunlaksananusorn, F. Rampf, L. Rodefeld, Organometallics 25 (2006) 2449;
(b) G.D. Frey, C.F. Rentzsch, D. von Preysing, T. Scherg, M. Mühlhofer, E. Herdtweck, W.A. Herrmann, J. Organomet. Chem. 691 (2006) 5725.
[23] (a) M.D. Sanderson, J.W. Kaupain, C.W. Bielawski, J. Am. Chem. Soc. 128 (2006) 16514;
(b) J. Barluenga, R. Vicente, l.A. López, M. Tomás, J. Organomet. Chem. 691 (2006) 5642.
[24] O.V. Starikova, G.V. Dolgushin, L.I. Larina, P.E. Ushakov, T.N. Komarova, V.A. Lopyrev, Russ. J. Org. Chem. 39 (2003) 1467.
[25] (a) CRYSALIS Data Collection Software and Data Processing Software for Oxford Diffraction Xcalibur devices, Version 1.171, Oxford Diffraction Ltd., Oxfordshire, United Kingdom, 2005;
(b) Data Collection Software and Data Processing Software for Stoe IPDS 2T diffractometer, X-AREA, Version 1.26, Stoe & Cie, Darmstadt, Germany, 2004;
(c) Data Processing Software for Stoe IPDS 2T diffractometer, XRED, XSHAPE, Version 1.26, Stoe & Cie, Darmstadt, Germany, 2004;
(d) A. Altomare, G. Cascarano, C. Giacovazzo, A. Guagliardi, M.C. Burla, G. Polidori, M. Camalli, J. Appl. Crystallogr. 27 (1994) 435;
(e)A.J.C. Wilson (Ed.), International Tables for Crystallography, vol. C, Kluwer Academic Publishers, Dordrecht, The Netherlands, 1992, Tables 6.1.1.4, 4.2.6.8, and 4.2.4.2;
(f) G.M. Sheldrick, SHELXL-97, Universität Göttingen, Göttingen, Germany, 1998;
(g) A.L. Spek, PLATON, A Multipurpose Crystallographic Tool, Utrecht University, Utrecht, The Netherlands, 2001;
(h) L.J. Farrugia, J. Appl. Crystallogr. 32 (1999) 837.